Investigation of a novel technique for the detection of electrophysiological/biophysical differences in bacterial cultures, using high-frequency, dielectric spectroscopy

Mohammad Russel[a,*], Sophocleous Marios[b], Shan JiaJia[a], Weiping Xu[a], Lehui Xiao[c], Thomas Maskow[d], Md. Mahbub Alam[e], Julius Georgiou[b]

[a] School of Food and Environment, Key laboratory of Industrial Ecology and Environmental Engineering, Ministry of Education, Dalian University of Technology, Panjin 124221, PR China

[b] Holistic Electronics Research Laboratory, Department of Electrical and Computer Engineering, University of Cyprus, Kallipoleos 75, 1678 Nicosia, Cyprus

[c] College of Chemistry, Nankai University, Tianjin, 300071, PR China

[d] UFZ, Helmholtz Centre for Environmental Research, Department of Environmental Microbiology, Permoserstr. 15,04318 Leipzig, Germany

[e] Institute for Turbulence-Noise-Vibration Interaction and Control, Shenzhen Graduate School, Harbin Institute of Technology, Shenzhen, China

ABSTRACT

The paper describes a novel technique to quantify and qualify bacterial cultures (*Bacillus Subtilis* and *Escherichia Coli*) in corn oil using dielectric spectroscopy at elevated frequencies (0.0100-20.0 GHz). This technique is using the electrophysiological/biophysical differences (e.g. gram positive and gram negative) between various bacteria types, as a basis to distinguish between bacteria concentrations and bacteria types. A close-ended, coaxial probe (20.0 mm long sample holder) was developed and used to calculate the dielectric constant of the bacterial cultures using the Nicolson-Ross-Weir method. This technique shows a linear relationship between the dielectric constant and the cell concentration, at 16.0 GHz. The sensitivity is 0.177 x 10^9 (CFU mL^{-1})$^{-1}$ for *B. Subtilis*, 0.322 x 10^9 (CFU mL^{-1})$^{-1}$ for *E. Coli* and 0.913 x 10^9 (CFU mL^{-1})$^{-1}$ for their 1:1 mixture, while the response time is 60.0s. The dependency of dielectric constant on the bacterial cell concentration at a given frequency, can be potentially exploited for measuring bacterial concentrations and biophysical differences.

Keywords: Dielectric spectroscopy, Complex permittivity, Bacterial Monitoring, Pathogen monitoring.

---

*Corresponding author.

Email address: mrussel@dlut.edu.cn (M. Russel)

1. Introduction

The rapid and reliable detection and identification of pathogenic microorganisms is of increasing importance mainly in the food industry, water supply, environment quality control and clinical diagnosis [1]. In particular, biosensors are of interest for the detection and identification of biomolecules [2-7], viruses [8], and bacteria [9-11]. The most influential advantage of biosensors is often their simplicity of operation, which makes them valuable tools in biomedical assays, environmental monitoring, bioprocess control, food safety, and national security among others. Biosensors can often be easily used by personnel with minimal training and do not normally require complex sample preparation or separation schemes for analysis. They often provide a high specificity and sensitivity making them of great interest in bio-detection [12, 13].

Food industry is maybe the area with the highest interest in the application of biosensors. Non-detection or late detection of bacterial contaminations in food, can have fatal consequences making direct countermeasures impossible. Six reviews published only in the period 2008-2009, indicate the critical importance of bacterial detection. The reviews were dealing with electrochemical biosensors for food pathogens [14], applications of microarrays in pathogen detection and biodefence [15], traditional pathogen detection methods [16], on-site pathogen detection using antibody-based sensors [17] and electrochemical impedance sensors for rapid detection of foodborne pathogenic bacteria [13, 18].

Traditional methods to quantify bacteria are the colony counting measurements using colony forming units (CFU), polymerase chain reactions (PCR) and

immunological assays. These techniques are often laborious and take a minimum of 7 days to follow the standard procedures [19]. On the other hand, immunological techniques need expensive chemicals and complicated steps involving sample preparations [20, 21]. The nucleic acid, probe-based methods are quite costly and need very highly specialised infrastructure [22]. However, all of these techniques have their limitations, such as non-viable cells and single-naked DNA, involve extraction and degradation of nucleic acids whilst the direct inhibition of the PCR may lead to false positive/negative responses [23]. Therefore, in this work a dielectric spectroscopic method is presented, which is a simple and label-free technique to identify and quantify bacterial cultures.

Dielectric properties (complex permittivity) of materials have received growing attention along with the use of electromagnetic waves (EM) (radar/microwave) in the investigations of material and structural assessment. Dielectric properties of a material correlate to other material characteristics and may be used to determine properties such as moisture content, bulk density, content of biological material, and chemical composition [24]. Dielectric spectroscopy [25-35] has already been proven to be a useful tool for the estimation of the biomass concentrations of many different microbial strains [36-44]. The simplest version of the method is based on the magnitude assessment of the β-dielectric dispersion at the radio frequency (RF) range exhibited by practically, all intact cells. The cells behave like a tiny capacitor and the signal correlates linearly with the volume-fraction of biomass. This linearity is lost above very high levels of biomass concentrations. Gopal Kedia and Thomas in their papers from

2013 and 2008, have shown that the high accumulation of lipid droplets and polyhydroxyalkanoates are the few exceptions to the rule [45-47].

In circuits with frequencies within the radio and microwave range, the circuit capacitance increases and conductance decreases, as the concentration of biological material increases. That frequency dependency is called the β-dielectric dispersion. Charges are unable to cross the cell membrane at low frequency range, due to the insulation of the conducting cytoplasm, which results in large macroscopic capacitance. The dielectric increment of a cell suspension from high to low frequencies, is therefore dependent on the volume fraction of biomass, the cell size and the membrane capacitance per unit area. Also, the conductivity of the suspension has an effect on the permittivity measured at a particular frequency [13, 38], but this effect can be minimized by the choice of the right frequencies.

In this work, a novel biophysical method is demonstrated, to measure the dielectric properties of bacterial cultures by a close-ended, coaxial, air-line probe at microwave frequencies. The data obtained with this technique are in-line with the results from scanning electron microscopy (SEM). For the exemplification of the method, *Escherichia coli (E. Coli)* and *Bacillus Subtilis* (*B. Subtilis*) were chosen for the experiments.

2. Background Theory

The fundamental concept of high-frequency network analysis involves incident, reflected and transmitted waves travelling along transmission lines. It is helpful to think of travelling waves along a transmission line, in terms of a light wave analogy. We can

imagine an incident light wave striking some optical component e.g. a lens. A fraction of the light is reflected off the surface of the lens, but most of it passes through the lens. If the lens was made from some lossy material, then a portion of the light could be absorbed within the lens. If the lens had mirrored surfaces, most of the light would have been reflected and little or none would have been transmitted through the lens. This concept is also valid for RF signals since they are also electromagnetic waves. The components and circuits are electrical devices and networks, instead of lenses and mirrors [48].

Network analysis is concerned with the accurate measurement of the ratios of the reflected and transmitted signal to the incident signal. This measurement is possible with the prototype probe shown in Figure 1. Looking at the transmitted and reflected wave data, the dielectric properties of the *E. Coli* and *B. Subtilis* cultures, as well as of several reference materials, can be investigated.

Figure 1.

The electromagnetic parameters can be deduced from the scattering parameters [49-52]. The boundaries of the material (Air and Teflon were used as low-loss materials) under test (MUT) are pre-defined and the S parameters can be accurately determined [53]. The following equations show the relationship between the parameters S_{11} (scattering parameter related to the radiation emission from port 1 and collected in port 1) and S_{21} (scattering parameter related to the radiation emission from port 1 and collected in port 2) (Figure S1) with the reflection and transmission coefficients Γ and T, respectively. These equations provide the solution for the boundary-condition

problem at L = 0 m (L is the line of air) and 20.0 mm = d (d is the sample thickness), such that the reflection coefficient can be expressed as [50, 51]:

$$\Gamma = X \pm \sqrt{X^2 - 1} \tag{1}$$

Where:

$$X = \{S_{11}^2(\omega) - S_{21}^2(\omega)\} + \frac{1}{2} S_{11}(\omega) \tag{2}$$

The transmission coefficient is given by:

$$T = \{S_{11}(\omega) + S_{21}(\omega)\} - \frac{\Gamma}{L} - \{S_{11}(\omega) + S_{21}(\omega)\}\Gamma \tag{3}$$

From Equations 1 and 2, the auxiliary variables (X and Y) are defined as follows:

$$X = \frac{\mu_r}{\varepsilon_r} = \left(\frac{1+\Gamma}{1-\Gamma}\right)^2 \tag{4}$$

$$Y = \mu_r \times \varepsilon_r = \left\{\frac{c}{\omega d} \ln\left(\frac{1}{T}\right)\right\}^2 \tag{5}$$

$$\mu_r = \sqrt{XY} \tag{6}$$

$$\varepsilon_r = \sqrt{\frac{Y}{X}} \tag{7}$$

Where:

c = speed of the light (m s^{-1});

μ_r = relative permeability of the material;

ε_r = relative permittivity of the material;

ω = angular speed (rads s^{-1});

One technique that uses the scattering parameters S_{11} and S_{21} to calculate the mentioned complex parameters of samples is named Nicolson-Ross-Weir (NRW) [51, 52]. The NRW modelling method is the most commonly used method to perform the calculation of complex permittivity and permeability of materials. This modelling

method has the advantage of being non-interactive, as required in the Baker-Jarvis method [54]. Furthermore, the NRW modelling method is applicable for coaxial line and rectangular waveguide cells. On the other hand, it is known that the NRW can diverge for low-loss materials at frequencies corresponding to integer multiples of one half wavelength in the sample [51, 52]. At this particular frequency, the magnitude of the measured S_{11} parameter is particularly smaller (thickness resonance) and the S_{11} phase uncertainty becomes larger. This behaviour can lead to the appearance of inaccuracy peaks on the permittivity and permeability curves.

This knowledge was used to investigate the complex permittivity and permeability of *E. Coli*, *B. Subtilis* and mixtures thereof, with the final goal to validate the electrophysiological differences and identify the bacterial cultures.

3. Materials and Methods

3.1. Micro-organism culturing

Bacillus Subtilis (TY453) and *Escherichia coli* (MN 675) were kindly provided by the State Key Laboratory of Agricultural Microbiology, College of Life Science and Technology, Huazhong Agricultural University (Wuhan, China). These bacteria were maintained at 4ºC on nutrient agar (Aobox biotechnology,02-024, Shanghai P.R.China) (NaCl 10.0 g L^{-1}, Peptone 10.0 g L^{-1}, Yeast extract powder 5.00 g L^{-1} and the pH was adjusted to 7.00) with 0.500% Pepton, before the electromagnetic measurement. Pre-cultures, were re-activated with NaCl 0.850 % and the growth dynamics study was prepared from 100 ml with added 1.00 ml stock cell seeds while further incubated in

Luria broth (LB, Beijing Solarbio Science & Technology Co.P.R.China, L8291, Tryptone 40.0 g L^{-1},Sodium chloride 40.0 g L^{-1},Yeast 20.0 g L^{-1}) for 24-48h at 37.0°C. The pellet was then transferred to selective agar medium and sub-cultured for 24-48h at 37.0°C in order to confirm the purity of the strains [55]. Characteristic colonies were transferred to non-selective broth and agar media, and cultured for 24-48h at 37.0°C. Colonies obtained in agar cultures were then transferred to Glycerol/Tryptic Soy Broth (TSB, Aobox biotechnology,02-102, Shanghai P.R.China, Tryptone 17.0 g L^{-1},Sodium chloride 5.00 g L^{-1},Disodium phosphate 2.50 g L^{-1},Glucose 2.50 g L^{-1}, Soybean papain hydrolyzate 3.00 g L^{-1}) at a 20:80 ratio and stored at -20.0°C until needed and reactivated by inoculating the bacteria in 10.0 ml of sterile broth medium at 37.0°C for 24h.

Selected bacteria were inoculated with 10.0 ml of sterile beef extract and peptone culture medium at 37.0°C for 24h for the bacteria enumeration assays, the electromagnetic measurements and the preparation of standard solutions. The resulting solution was diluted with 1:4 ratio to provide a series of stock solutions of bacteria. Serial dilution gradients of *Bacillus Subtilis* and *Escherichia coli* overnight cultures were prepared by performing electromagnetic measurement until the observed particle concentration was close to the specified detection limit of 10^9 CFU mL^{-1}. For *Bacillus Subtilis*, 6 steps of two-fold serial dilutions were performed, reaching an overall dilution of 128-fold. For *Escherichia Coli*, eight steps of two-fold serial dilution were performed, finally reaching a final 512-fold dilution. Measurements were repeated three times using three independently prepared serial dilution gradients. The bacteria samples were

centrifuged at 6000 RPM for 15.0 minutes and the supernatant was discarded. The precipitate was injected in 1.50 ml of corn oil. Each stock solution was quantified three times with the standard plate count method [56] in the appropriate culturing agar medium (e.g. beef extract and peptone medium for *E. Coli* and *B. Subtilis* respectively).

3.2. Instrumentation

An automatic vector network analyser (VNA, Agilent E8362B, Shanghai, China) with frequency range of 0.0100-20.0 GHz was connected with a custom-made, coaxial, air-line probe (20.0 mm long) as shown in Figure 2 for experimentation of bacterial cultures at room temperature (25°C).

The construction of the coaxial, air-line probe is shown in more detail in Figure 1.

Figure 2.

The most important factors for the dielectric properties of the solutions are concentration, polarity, size and geometry of the bacteria under investigation. For *B. Subtilis* 1.30, 1.50, 1.80, 2.10 x 10^9 CFU mL^{-1} concentrations were used, while for *E. Coli* 1.00, 1.20, 1.40, 1.60 x 10^9 CFU mL^{-1} concentrations were used. The size of bacteria was 10.0 x 1.00 μm and 2.00 x 0.50 μm respectively whilst rod-like/ellipsoidal shapes have been chosen for further measurement at 25.0°C.

Scanning electron microscopy was performed for the determination of the latter two parameters. SEM scans of pure and mixed cultures of *E. Coli* and *B. Subtilis* for 2.10 x 10^9 CFU mL^{-1} concentration have been performed using a FEI SIRION scanning electron microscope (Amsterdam, Netherland) at 25.0°C.

3.3. Experimental Procedure

The bacterial cultures were suspended in corn oil to reduce the influence of the solvent on the dielectric behaviour of the suspension. The frequency range was 0.0100–20.0 GHz and the applied coaxial air-line probe was 20.0 mm long. The experimental procedure is shown in Figure 3. Firstly, the corn oil and different concentrations of *B. Subtilis* and *E. Coli* suspension were prepared. Then, the coaxial probe cavity cell was filled using 1.50 ml of corn oil and measured their reflection (S_{11}) and Transmission (S_{21}) value at 25.0^{o}C, since corn oil's S parameters will work as a reference material. The second step was to inject the different concentrations of *B. Subtilis* and *E. Coli* suspended broth, into the corn oil and finally measure their S parameters (S_{11} and S_{21}) to calculate their complex permittivity and permeability using the NRW model.

The instrument was regularly calibrated with short-open-50Ω load-through (Maury Microwave, model 8050CK11) techniques, to move the reference plane to the end of the test cables. The probe was using a phase-shift approach from reference plane to surface plane ($\Delta\phi_1$ and $\Delta\phi_2$), as shown in Figure 4.

Figure 3.

Figure 4.

To determine the complex permittivity and permeability, via S-parameters (S_{11} and S_{21}), the two-port transmission and reflection techniques were used, for a material-under-test (our microbe sample) with smooth flat faces, and filling completely the fixture cross-section (Figure 1, cell cavity), being placed inside a coaxial, air-line probe. The two-port transmission and reflection S-parameter data were measured in the test frequency range of 0.0100-20 GHz and 801 data points were taken for each sweep. To

minimize the systematic measurement noise errors, a 32.0-point averaging factor was chosen in the VNA system.

TEM propagation mode was used for the coaxial, air-line probe to measure the reflection and transmission scattering parameters S_{11} and S_{21}. Transverse electromagnetic mode (TEM) means that the particular electromagnetic field pattern of radiation is measured in a plane perpendicular (i.e., transverse) to the direction of travel of the radiation. The measured data was inserted in Origin 8 software (USA) and Equations 8 & 9 were used to get accurate scattering parameters from the sample surface plane. Here, these simple algorithms (Equations 8 & 9) were used to correct the phase shift (Δφ) for frequency f [57] .

$$\Delta\varphi_{11} = 2\,a\,\frac{2\,\pi\,f}{c} \quad for \quad S_{11} \tag{8}$$

$$\Delta\varphi_{21} = (a+b)\,\frac{2\,\pi\,f}{c} \quad for \quad S_{21} \tag{9}$$

Where:

c = speed of light (m s^{-1})

a, b = distances from sample surface (m)

The phase shift correction approach is shown in Figure 4. After determination of the S-parameters, the complex parameters (ε_r and μ_r) were calculated according to the NRW modelling method.

3.4. Numerical Simulations

For the calculation of permittivity and permeability of the samples, numerical simulations were used. Figure 5 shows the respective flowchart. The complex

parameters for air were taken from literature (ε_r = 1.0-0.0j and μ_r = 1.0-0.0j) [58]. Based on the complex parameters from literature [59] and on the scattering matrix defined in this study, the coaxial, air-line probe tool was used to simulate the scattering parameters S_{11} and S_{21} of the air sample (control experiment at 25.0 °C). Afterwards, using the magnitude and phase values of the simulated parameters, the complex parameters were retrieved according to Figure 5.

Figure 5.

4. Results and Discussion

4.1. Investigation of the dielectric constant of pure bacterial strains at various frequencies

Initially, the relationship between the calculated dielectric constant and frequency was investigated for pure bacterial strains. *B. Subtilis* cells were injected in corn oil at different concentrations (1.30, 1.50, 1.80 and 2.10 x 10^9 CFU mL^{-1}) and the medium was then tested using the prototype probe. The exact same procedure was followed for *E. Coli* (1.00, 1.20, 1.40, 1.60 x 10^9 CFU mL^{-1}) and the results are presented in Figure 6.

Figure 6.

Figure 6 shows that the dielectric constant of the MUT decreases with increasing frequency. Initially, the dielectric constant changes rapidly but at higher frequencies it tends to stabilise. The plots follow a decaying profile but that profile is very similar for different cell concentrations. It is clear that the graph is shifted upwards as the cell

concentration increases. That shift is larger for *B. Subtilis* than it is for *E. Coli*. The shift between different concentrations of the same bacteria looked constant and therefore, it was suspected that the relationship between the dielectric constant and cell concentration at a specific frequency would be linear.

4.2. The relationship between the dielectric constant and cell concentration

In order to show the relationship between the dielectric constant and the cell concentration, a frequency range of 15.0-16.0 GHz was chosen, since this is where the frequency graphs tend to flat out. In this set of experiments, a mixture of the two bacteria types was also investigated. The mixture was made up with 1:1 ratio at various concentrations. The results are shown in Figure 7.

Figure 7.

Figure 7 shows the relationship between the dielectric constant (ε_r) and bacteria cell concentrations (*10^9 CFU/mL). There is a linear relationship between the ε_r and bacteria concentration for *E. Coli*, *B. Subtilis* and the mixture for the two. It was found that the dielectric constant of the mixture is sitting on the top of the *B. Subtilis* and *E.coli* at the frequency range 15.0-16.0 GHz. From their slope intercept analysis, it is clear that the slope of the mixture is the highest, *E. Coli* is the second highest and *B.subtilis* shows the lowest slope. All three graphs have an r^2 value of more than 0.999. The gradients of the graphs show the sensitivity of the probe for bacteria cell concentration in corn oil. The absolute values of the dielectric constant for *B. Subtilis* are lower than *E. Coli* while the mixture has again the highest values. The sensitivity is for *B. Subtilis* is 0.177 x 10^9 (CFU $mL^{-1})^{-1}$, 0.322 x 10^9 (CFU $mL^{-1})^{-1}$ for *E. Coli* and

0.913 x 10^9 (CFU mL^{-1})$^{-1}$ for the 1:1 mixture, respectively. Although the minimum concentrations of bacteria to be detected were too high compared to other available methods, available microfluidic platforms can locally enrich bacteria concentrations to the levels of detection [13, 60-62]. It is believed that more kinds of pathogens/bacteria can be detected with this method, but it will depend on the biophysical and electrophysiological properties of each pathogen. This is part of future work by the same group. Therefore, this approach could be very promising to determine the biosafety and biosecurity issues in the future.

4.3. Forward scattering magnitude and selectivity of pure and mixed bacteria cultures

In order to understand the reasons of the higher sensitivity for the mixture of the two bacteria types, the magnitude of the transmitted wave was investigated using the complex parameter's S_{21} real and imaginary values (at cell concentration 2.10 x 10^9 CFU mL^{-1}). S_{21} represents the transmission coefficient, which is a measure of the magnitude of the wave that was transmitted through the bacterial cell broth. It was found that the magnitude of S_{21} is affected from the presence of microbial cells showing similar behaviour. A microbe concentration of 2.10 x 10^9 CFU mL^{-1} was used for pure strains and the mixture of the two in corn oil.

Figure 8.

It was found that the corn oil's interference is very low -0.067dB (Figure 8), which is negligible. On the other hand, single strains show a higher dB degradation than pure corn oil, of approximately -5.54 dB & -12.33 dB for *E. Coli* and *B. Subtilis,* respectively.

The mixture shows an even higher degradation of approximately -37.7 dB. Those degradation values appear around 16.0 GHz for all mediums.

Bacterial cell surfaces are generally, in possession of polysaccharides and S-layer glycoproteins while their cell membrane possesses lipid bilayers with a characteristic cytoplasmic electrophysiology arising from water within different bound forms. This functional groups' diversity is associated with the characteristic differences of their net conductivity. The key reason to have higher electrical conductivity in Gram-positive bacteria is because of their prominent cell wall and absence of outer lipid membrane layer [13]. Based on their physico-chemical properties, *E. Coli* is gram-negative and *B. Subtilis* is gram-positive. *B. Subtilis* shows higher dB degradation than the *E. Coli* due to above reason. The gram positive or negative bacterial electrical conductivity could vary with their shape, composition, and geometry of each sub-cellular layer, where they get the opportunity for selective polarization. More specifically, it could vary as a function of the amplitude of the applied field, the frequency and the opposing flow fields.

The strain mixture shows a higher dB degradation, most probably due to their larger surface area compared to the single microbial cell. The net particle conductivity found for *Bacillus subtillis* is 935 ±96.0 μS cm^{-1} and *Escherichia coli* 412 ±25.0 μS cm^{-1}. The shape of both bacteria types is rod-like shape or ellipsoidal, but their dimensions for *Bacillus subtillis* and *Escherichia coli* is 10.0 x1.00 and 2.00 x 0.50 respectively [63]. A couple of studies have found that the bacterial shapes or dimensions are major factors related to their conductivity. For example, *Lactococcus lactis* and

Saccharomyces cerevisiae are both gram-positive and their shapes are spherical with dimensions and net particle conductivity of 1.20 x 1.00 μm and 416 ±46.0 μS cm^{-1}, 4 μm in diameter and 16 μS cm^{-1}, respectively [64,65]. The bacterial cell wall also contributes to the conductivity. Gram-positive bacterial cell wall is 50.0-70.0 nm thick with highly charged peptidoglycan structure and densely anionic glycopolymers. On the other hand, gram-negative bacteria cell wall is 8.00-10.0 nm and the cell surface is made up of carboxylic acids and phosphate groups, mostly phospholipids, membrane proteins and lipopolysaccharides. These induce negative charges to the surface that leads to minimizing their conductivity [13].

In terms of selectivity, *B. Subtilis* and *E. Coli* show very different electrophysiological properties throughout the whole frequency range with respect to their magnitude (dB) degradation. At this stage, only gram positive and gram negative bacterial types can be easily identified at a particular frequency, but further investigation is required to consider all other chemical and physical properties of bacteria in an attempt to use this method for identification of other bacteria types. The magnitude of S_{21} spectra can possibly work as a fingerprint of their physico-chemical properties.

4.4. Morphological and Media conductivity investigation of different bacteria strains

In order to better understand the reasons of these differences on the dielectric constant of different bacterial cultures, SEM scans were performed. Figure 9 shows images from the SEM scans for all bacteria culture combinations.

Figure 9.

Both pure strains have very similar rod-shape/ellipsoidal shape. However, *E. Coli* is approximately 2.00 x 0.50 μm in size while *B. Subtilis* is 10.0 x 1.00 μm. It is believed that cell size is the determining factor for the differences in the magnitude of S_{21}. As it was discussed in the previous section, the ellipsoidal shape could have larger surface compared to spherical shape. Therefore, due to the larger surface area bacteria will have higher net particle conductivity. Differences in surface area combined with difference in gram-strain could influence the S_{21} magnitude between different types of bacteria. In the case of the mixed bacteria culture, the cells possess different polarities. It is shown in literature that the amplitude of externally applied voltage and the degree of non-uniformity in electric field are the determining factors for the magnitude of the dielectric values while media conductivity plays a very important role. The frequency-dependent difference of complex permittivity of the particle and its surrounding media, determines the direction of particle translation. Hence, particles that are more polarizable than the surrounding media are shifted towards the high-end of dielectric values. On the other hand, if the particles are less polarizable than the surrounding media, they are shifted towards the low field region [13]. Therefore, to optimize the media conductivity, a similar type of oil was tested (paraffin oil), which has a dielectric value of $3.13 \pm 4.40 \times 10^4$ while corn oil has $2.20 \pm 4.40 \times 10^4$ at 25.0°C [66]. It was found that, the corn oil has less ionic polarization and smother electromagnetic signal response, than the paraffin oil (Fig. 10). From Fig 10, it is clearly observed that the magnitude degradation of paraffin oil is quite unstable compared to corn oil although, the average

magnitude degradation for paraffin is -1.56 dB and corn oil -2.53 dB. Therefore, corn oil was selected as a matching microfluidic platform to study the bacterial cell dielectric constant.

As explained earlier, *B. Subtilis* is gram-positive and *E. Coli* is gram-negative. *B. Subtilis* has significantly higher net particle conductivity due to higher surface area and thicker cell wall compared to *E. Coli*. That is probably the reason for the significant magnitude degradation of *B. Subtilis* compared to *E. Coli*. Therefore, the assumption made was that, it could be linked with the gradual reduction of cytoplasm polarizability for these respective strains, as we know their dimensional size, shapes and thickness of cell wall are identical [13,67]. It is well-known that cytoplasmic polarizability of bacterial cells could be observable in high frequency range study [13]. That is consistent with S_{21} magnitude degradation study at 16.0 GHz (Figure 8). Assuming that cytoplasmic polarizability of bacterial cells is connected with the cationic and anionic functional groups of the molecules in the bacterial cell wall, the size difference is large enough to explain the S_{21} magnitude differences observed. The results from the SEM study in Figure 9 show a clear image of their dense bondage. The evaluation of all potential reasons for the different behaviour of the pure and mixed cultures is outside of the goal of this study. However, the discussed reason is maybe already enough so that the dielectric permittivity and the magnitude of forward scattering could act as a fingerprint signature of bacterial cells and would be suited to differentiate between different species to a certain extent.

5. Conclusions

A close-ended, coaxial, air-line probe has successfully been constructed and used to investigate the dielectric behaviour of various bacterial cultures (*E. Coli*, *B. Subtilis* and their mixtures). It was demonstrated that the electromagnetic properties at frequencies between 0.0100–20.0 GHz have the potential to be applied to identify bacterial contaminations. It is possible, to a certain extent, to differentiate between different bacterial species and the method can possibly extrapolate to bacterial electrophysiological differences. The main advantage of the proposed method is the speed of analysis with the use of microfluidic methods, where bacteria concentrations can be locally enriched to these levels for detection. The relationship of the dielectric constant and cell concentration is proven to be linear with r^2 values higher than 0.999 for all tested mediums while the sensitivity of the system is 0.177 x 10^9 $(CFUmL^{-1})^{-1}$ for *B. Subtilis,* 0.322 x 10^9 $(CFU\ mL^{-1})^{-1}$ for *E. Coli* and 0.913 x 10^9 $(CFU\ mL^{-1})^{-1}$ for their mixture, respectively. The response time of the process is 60.0s. Both analytical parameters can be improved by redesigning the inner core diameter and outer core diameter of the probe. The proposed method could give a new forge direction to environmentalists and biologists for a more economic and less time-consuming bacterial detection method.

Acknowledgements

This work was supported by the National Natural Science Foundation of China (41603069) and the fundamental Research Funds for the Central Universities grants from Dalian University of Technology (Panjin campus) .

References

[1] O. Lazcka, F.J. Del Campo, F.X. Munoz, Pathogen detection: a perspective of traditional methods and biosensors, Biosens. Bioelectron. 22 (2007) 1205-1217.

[2] N.W. Downer, L. Jianguo, E.M. Penniman, L.W. DeLuca, H.G. Smith, Surface-bound biomembranes incorporating receptors: electrochemical and structural characterization, Biosens. Bioelectron. 7 (1992) 429-440.

[3] Y.-Z. Du, S.S. Saavedra, Molecular orientation distributions in protein films. V. Cytochrome c adsorbed to a sulfonate-terminated, self-assembled monolayer, Langmuir. 19 (2003) 6443-6448.

[4] E. Kress-Rogers, Handbook of biosensors and electronic noses: medicine, food, and the environment, CRC Press1996.

[5] A. Perrin, V. Lanet, A. Theretz, Quantification of specific immunological reactions by atomic force microscopy, Langmuir. 13 (1997) 2557-2563.

[6] R. Parthasarathy, T. Globus, T. Khromova, N. Swami, D. Woolard, Dielectric properties of biological molecules in the Terahertz gap, Appl. Phys. Lett. 87 (2005) 1130901-1-3.

[7] D. K. George, A. Charkhesht, N. Q. Vinh, New terahertz dielectric spectroscopy for the study of aqueous solutions, Rev. Sci. Instrum.86 (2015) 123105-1.

[8] W.W. Tourtellotte, P. Schmid, P. Pick, N. Verity, S. Martinez, P. Shapshak, Quest for a reliable, valid, and sensitive in situ hybridization procedure to detect viral nucleic

acids in the central nervous system, Neurochem. Res. 12 (1987) 565-571.

[9] S.W. Howell, H.D. Inerowicz, F.E. Regnier, R. Reifenberger, Patterned protein microarrays for bacterial detection, Langmuir. 19 (2003) 436-439.

[10] C. Ruan, L. Yang, Y. Li, Immunobiosensor chips for detection of Escherichia c oli O157: H7 using electrochemical impedance spectroscopy, Anal. Chem. 74 (2002) 4814-4820.

[11] K. Seo, R. Brackett, N. Hartman, D. Campbell, Development of a rapid response biosensor for detection of Salmonella typhimurium, J. Food Prot. 62 (1999) 431-437.

[12] M. Mehta, C.S. Hanumanthaiah, P.A. Betala, H. Zhang, S. Roh, W. Buttner, W.R. Penrose, J.R. Stetter, V.H. Pérez-Luna, Detection of proteins and bacteria using an array of feedback capacitance sensors, Biosens. Bioelectron. 23 (2007) 728-734.

[13] R. E. Fernandez, A. Rohani, V. Farmehini, Review: Microbial analysis in dielectrophoretic microfluidic systems, Anal. Chim. Acta. 966 (2017) 11-33.

[14] O.A. Sadik, A.O. Aluoch, A. Zhou, Status of biomolecular recognition using electrochemical techniques, Biosens. Bioelectron. 24 (2009) 2749-2765.

[15] M. Uttamchandani, J.L. Neo, B.N.Z. Ong, S. Moochhala, Applications of microarrays in pathogen detection and biodefence, Trends in biotechnology, 27 (2009) 53-61.

[16] I. Palchetti, M. Mascini, Electroanalytical biosensors and their potential for food pathogen and toxin detection, Anal. Bioanal. Chem. 391 (2008) 455-471.

[17] P.D. Skottrup, M. Nicolaisen, A.F. Justesen, Towards on-site pathogen detection using antibody-based sensors, Biosens. Bioelectron. 24 (2008) 339-348.

[18] L. Yang, R. Bashir, Electrical/electrochemical impedance for rapid detection of foodborne pathogenic bacteria, Biotechnol. Adv. 26 (2008) 135-150.

[19] E. D. Boer, R. R. Beumer, Methodology for detection and typing of foodborne microorganisms, Int. J. Food Microbiol. 50 (1999) 119-130.

[20] R. R. Beumer, E. Brinkman, Detection of Listeria spp. with a monoclonal antibody-based enzyme-linked immunosorbent assay (ELISA), Food Microbiol. 6 (1989) 171-177.

[21] J. D. Palumbo, M. K. Borucki, R. E. Mandrell, L. Gorski, Serotyping of Listeria monocytogenes by enzyme-linked Immunosorbent assay and identification of mixed-serotype cultures by colony immunoblotting, J. Clin. Microbiol. 41 (2003) 564-571.

[22] H. Y. Cai, J. L. Caswell, J. F. Prescott, Nonculture Molecular Techniques for Diagnosis of Bacterial Disease in Animals: A Diagnostic Laboratory Perspective, Veterinary Pathology, 51 (2014) 341-350.

[23] I. G. Wilson, Inhibition and facilitation of nucleic acid amplification, Appl. Environ. Microbiol. 63 (1997) 3741-3751.

[24] O. Büyüköztürk, T.-Y. Yu, J.A. Ortega, A methodology for determining complex permittivity of construction materials based on transmission-only coherent, wide-bandwidth free-space measurements, Cem. Concr. Compos. 28 (2006) 349-359.

[25] C. Davey, DB Kell in M. O'Connor, RHC Bentall and JS Monahan (Eds.), Emerging Electromagnetic Medicine, Springer, Berlin, 1990.

[26] K. Foster, H. Schwan, CRC Handbook of Biological Effects of Electromagnetic Fields, (1986).

[27] K.R. Foster, H.P. Schwan, Dielectric properties of tissues, Handbook of biological effects of electromagnetic fields, 2 (1995) 25-102.

[28] E.H. Grant, R. Sheppard, G. South, Dielectric behaviour of biological molecules in solution, Clarendon Press1978.

[29] D. Kell, Biosensors. Fundamentals and Applications.: APF Turner, I. Karube and GS Wilson, Oxford University Press, Oxford, 1987, ISBN 0-19-854724-2, xvi+ 770 pp., Elsevier, 1988.

[30] D.B. Kell, Determination of biomass, Google Patents, 1990.

[31] D.B. Kell, C.M. Harris, Dielectric spectroscopy and membrane organisation, Journal of Bioelectricity, 4 (1985) 317-348.

[32] R. Pethig, Dielectric and electrical properties of biological materials, Journal of Bioelectricity, 4 (1985) vii-ix.

[33] R. Pethig, D.B. Kell, The passive electrical properties of biological systems: their significance in physiology, biophysics and biotechnology, Phys. Med. Biol. 32 (1987) 933.

[34] O.F. Schanne, P. Ruiz, E. Ceretti, Impedance measurements in biological cells, Wiley1977.

[35] S. Takashima, Electrical properties of biopolymers and membranes, A. Hilger1989.

[36] C. Boulton, P. Maryan, D. Loveridge, D. Kell, The application of a novel biomass sensor to the control of yeast pitching rate, Proc 22nd Eur Brew Conv Zurich European Brewing Convention, Oxford University Press, 1989, pp. 653-661.

[37] C.L. Davey, D.B. Kell, R.B. Kemp, R.J. Meredith, On the audio-and radio-

frequency dielectric behaviour of anchorage-independent, mouse L929-derived LS fibroblasts, J. Electroanal. Chem. Interfacial. Electrochem. 254 (1988) 83-98.

[38] C.M. Harris, R.W. Todd, S.J. Bungard, R.W. Lovitt, J.G. Morris, D.B. Kell, Dielectric permittivity of microbial suspensions at radio frequencies: a novel method for the real-time estimation of microbial biomass, Enzyme Microb. Technol. 9 (1987) 181-186.

[39] D.B. Kell, R.W. Todd, Determination of biomass, Google Patents, 1989.

[40] G.H. Markx, D.B. Kell, Dielectric spectroscopy as a tool for the measurement of the formation of biofilms and of their removal by electrolytic cleaning pulses and biocides, Biofouling. 2 (1990) 211-227.

[41] G.H. Markx, H.J. ten Hoopen, J.J. Meijer, K.L. Vinke, Dielectric spectroscopy as a novel and convenient tool for the study of the shear sensitivity of plant cells in suspension culture, J. Biotechnol. 19 (1991) 145-157.

[42] N.G. Stoicheva, C.L. Davey, G.H. Markx, D.B. Kell, Dielectric spectroscopy: a rapid method for the determination of solvent biocompatibility during biotransformations, Biocatalysis, 2 (1989) 245-255.

[43] A.M. Woodward, D.B. Kell, On the nonlinear dielectric properties of biological systems: Saccharomyces cerevisiae, Bioelectrochem. Bioenerg. 24 (1990) 83-100.

[44] D.B. Kell, G.H. Markx, C.L. Davey, R.W. Todd, Real-time monitoring of cellular biomass: methods and applications, Trends Anal. Chem. 9 (1990) 190-194.

[45] G. Kedia, P. Passanha, R.M. Dinsdale, A.J. Guwy, M. Lee, S.R. Esteves, Addressing the challenge of optimum polyhydroxyalkanoate harvesting: Monitoring

real time process kinetics and biopolymer accumulation using dielectric spectroscopy, Bioresour. Technol. 134 (2013) 143-150.

[46] T. Maskow, A. Röllich, I. Fetzer, J.-U. Ackermann, H. Harms, On-line monitoring of lipid storage in yeasts using impedance spectroscopy, J. Biotechnol. 135 (2008) 64-70.

[47] T. Maskow, A. Röllich, I. Fetzer, J. Yao, H. Harms, Observation of non-linear biomass–capacitance correlations: Reasons and implications for bioprocess control, Biosens. Bioelectron. 24 (2008) 123-128.

[48] S. Efrima, H. Metiu, Classical theory of light scattering by an adsorbed molecule. I. Theory, J. Chem. Phys. 70 (1979) 1602-1613.

[49] A.L. de Paula, M.C. Rezende, J.J. Barroso, Experimental measuremental measurements and numerical simulation of permittivity and permeability of teflon in X band, doi: 10.5028/jatm. 2011.03019410, Journal of Aerospace Technology and Management, 3 (2011) 59-64.

[50] A.S.f.T.a. Materials., ASTM D5568-1: Standard Test Method for measuring Relative Complex permittivity and Relative Magnetic Permeability of Solid Materials at Microwave Frequencies. , West Conshohoken, PA: ASTM,2001.

[51] A. Nicolson, G. Ross, Measurement of the intrinsic properties of materials by time-domain techniques, IEEE Trans. Instrum. Meas. 19 (1970) 377-382.

[52] W.B. Weir, Automatic measurement of complex dielectric constant and permeability at microwave frequencies, Proceedings of the IEEE, 62 (1974) 33-36.

[53] M. Russel, S. Zhenxiang, L. Changrui, Z. Hao, L. Lifen,S. Marios, Z. Yong,

Development of a detection method based on dielectric spectroscopy for real-time monitoring of meta-cresol contamination in beach-sand, Sens. Act. A. Phys.

[54] J. Baker-Jarvis, M.D. Janezic, J.H. Grosvenor Jr, R.G. Geyer, Transmission/reflection and short-circuit line methods for measuring permittivity and permeability, NASA STI/Recon Technical Report N, 93 (1992) 12084.

[55] C. Pope, J. Wilson, E.N. Taboada, J. MacKinnon, C.A.F. Alves, J.H. Nash, K. Rahn, G.W. Tannock, Epidemiology, relative invasive ability, molecular characterization, and competitive performance of Campylobacter jejuni strains in the chicken gut, Appl. Environ. Microbiol. 73 (2007) 7959-7966.

[56] P. Gerhardt, R. Murray, R. Costilow, E.W. Nester, W.A. Wood, N.R. Krieg, G.B. Phillips, Manual of methods for general bacteriology, (1981).

[57] K. Jose, V. Varadan, V. Varadan, Wideband and noncontact characterization of the complex permittivity of liquids, Microw. Opt. Technol. Lett. 30 (2001) 75-79.

[58] S.O. Nelson, Measurement of microwave dielectric properties of particulate materials, J. Food Eng. 21 (1994) 365-384.

[59] Y.-F. Chen, H.-W. Wu, Y.-H. Hong, H.-Y. Lee, 40 GHz RF biosensor based on microwave coplanar waveguide transmission line for cancer cells (HepG2) dielectric characterization, Biosens. Bioelectron. 61 (2014) 417-421.

[60] M. M. Al-Shalalfeh, T. A. Saleh, A. A. Al-Saadi, Silver colloid and film substrates in surface enhanced Raman scattering for 2-thiouracil detection, RSC Adv. 6 (2016) 75282-75292.

[61] B. Pastorino, X. D. Lamballerie, R. Charrel, Biosafety and Biosecurity in european

Containment Level 3 Laboratories: Focus on French Recent Progress and essential Requirements,Frontiers in public health, 5 (2017) 121.

[62] G. Kim , J. Moon, C.Y. Moh, J.G. Lim, A microfluidic nano-biosensor for the detection of pathogenic Salmonella, Biosens. Bioelectron. 67 (2015) 243-247.

[63] A. C. S.Yu, J. F. C.Loo, S. Yu, S. K. Kong, T. F. Chan, Monitoring bacterial growth using tunable resistive pulse sensing with a pore-based technique, Appl. Microbiol. Biotechnol. 98 (2014) 855-862.

[64]J. Farmer, F. Hickman-Brenner, in: A. Balows (Ed.), The Prokaryotes. A Handbook on the Biology of Bacteria: Ecophysiology, Isolation, Identification, Applications, Springer, New York, 1992, pp. 2952-3011.

[65] F. Sherman, Getting started with yeast, Methods Enzym. 350 (2002) 3-41.

[66] L. Z. Hu, K. Toyoda, I. Ihara, Dielectric properties of edible oils and fatty acids as a function of frequency, temperature, moisture and composition, J. Food Eng. 88 (2008) 151-158.

[67] Y. H. Su, C. A. Warren, R. L. Guerrant, N. S. Swami, Dielectrophoretic Monitoring and Interstrain Separation of Intact Clostridium difficile Based on Their S(Surface)-Layers, Anal.Chem. 86 (2014) 10855-10863.

Figure Captions

Figure 1. Construction of the coaxial, air-line probe (up) & the three sections of the probe (down). (OD_b is the diameter of the outer casing and ID_a is the diameter of the inner rod)

Figure 2. Experimental setup using the VNA and the coaxial air-line probe at 25.0°C.

Figure 3. Flow chart of the measurement and evaluation of the complex permittivity and permeability properties of microbes at 25.0°C.

Figure 4. Phase-shift correction approach.

Figure 5: Flow chart of the numerical simulation used for the complex permittivity and permeability calculation at 25.0°C.

Figure 6. Calculated dielectric constant of different concentrations at 25.0°C vs frequency: *B. Subtilis* (up), *E. Coli* (down).

Figure 7. Linear relationship between the dielectric constant and the respective bacterial concentration at frequencies between 15.0-16.0 GHz, at 25.0°C.

Figure 8. Study of the forward magnitude and voltage degradation of corn oil, *E. Coli*, *B. Subtilis* and mixture thereof (*E. Coli* 50%+ *B. Subtilis* 50%) at 2.10 x 10^9 CFU mL^{-1} cell concentration at 25.0°C.

Figure 9. SEM scans with 7-8 thousand times magnification of (a) *Bacillus Subtilis* (b) *Escherichia coli* and (c) Mixture of 50.0 % *B. Subtilis* + 50.0% *E. Coli* at 25°C.

Figure 10. Study of the forward magnitude and voltage degradation of corn and paraffin oil at room temperature (25°C).

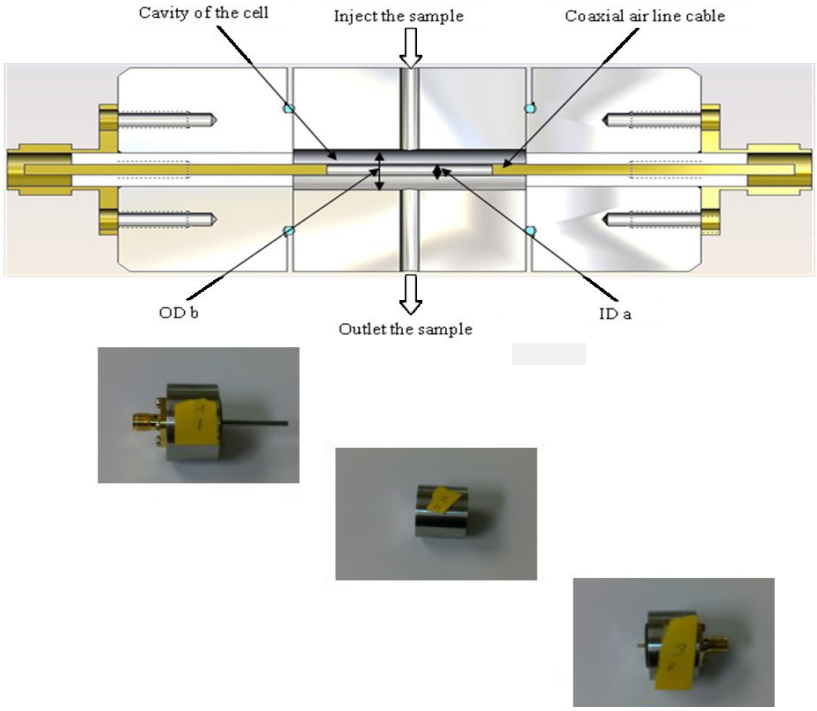
Cavity of the cell
Inject the sample
Coaxial air line cable
OD b
Outlet the sample
ID a

Figure 1

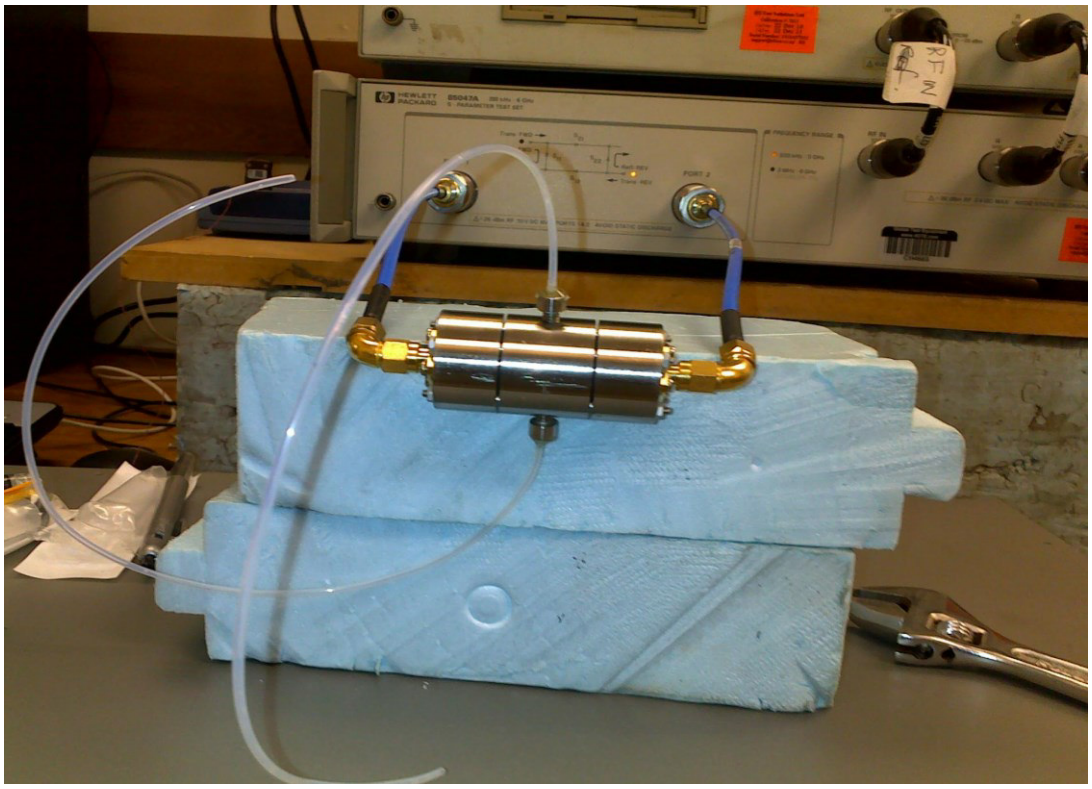

Figure 2

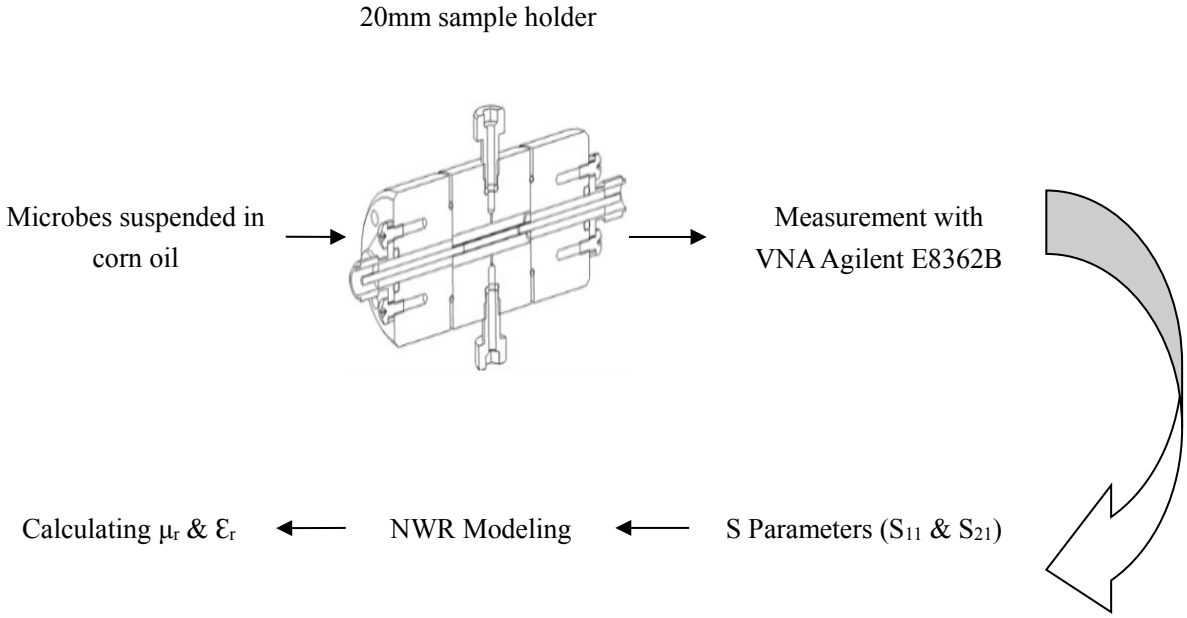
20mm sample holder
Microbes suspended in corn oil
Measurement with VNA Agilent E8362B
S Parameters (S_{11} & S_{21})
NWR Modeling
Calculating μ_r & ε_r

Figure 3

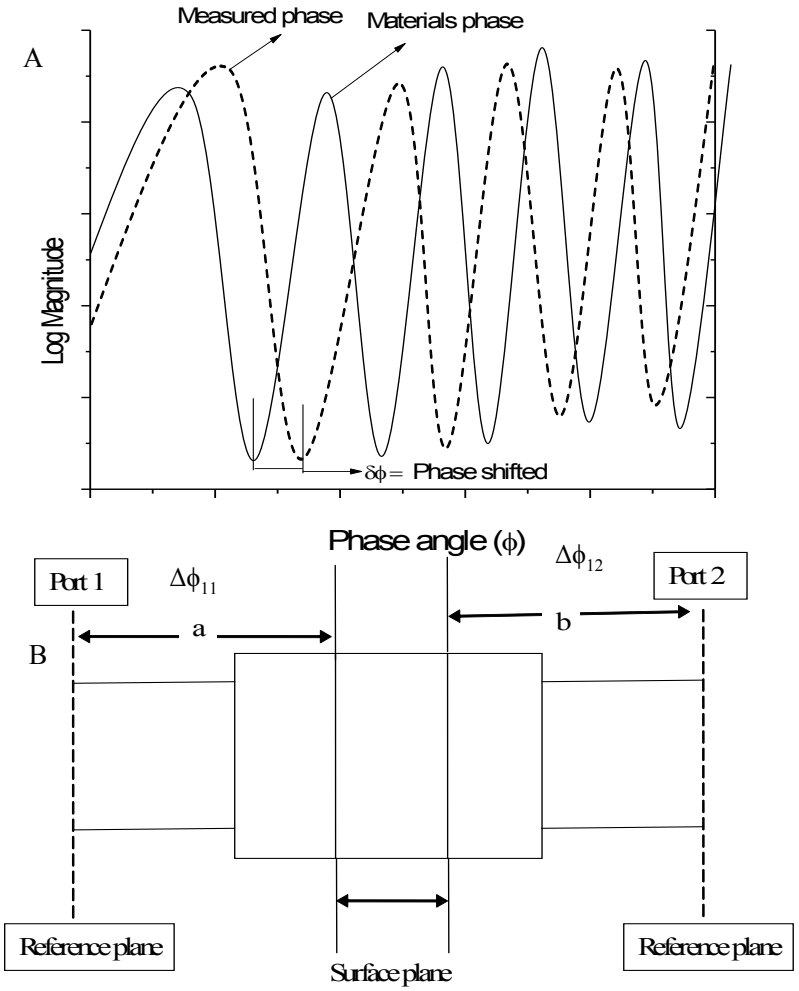
A
Measured phase
Materials phase
Log Magnitude
δϕ = Phase shifted
Phase angle (ϕ)
B
Port 1
Port 2
Δϕ11
Δϕ12
a
b
Reference plane
Reference plane
Surface plane

Figure 4

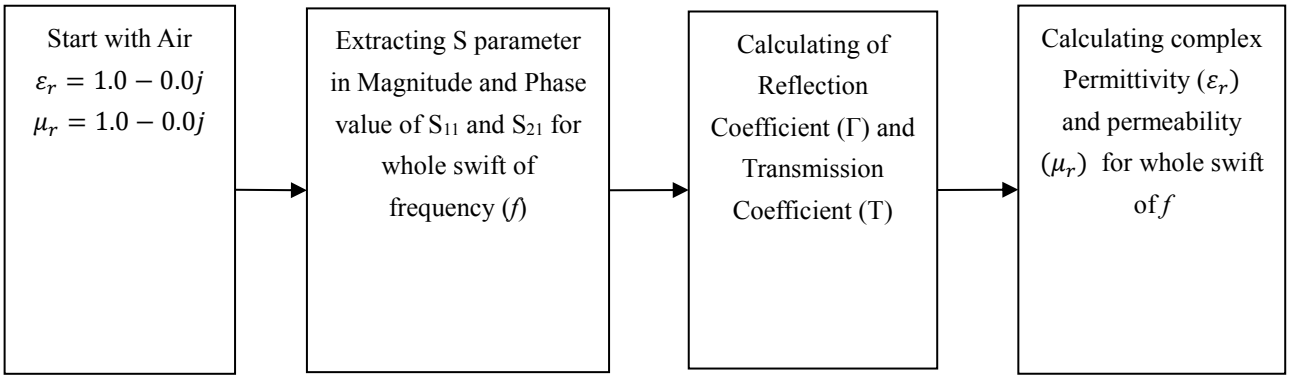
Start with Air
$\varepsilon_r = 1.0 - 0.0j$
$\mu_r = 1.0 - 0.0j$
Extracting S parameter in Magnitude and Phase value of S_{11} and S_{21} for whole swift of frequency (f)
Calculating of Reflection Coefficient (Γ) and Transmission Coefficient (T)
Calculating complex Permittivity (ε_r) and permeability (μ_r) for whole swift of f

Figure 5

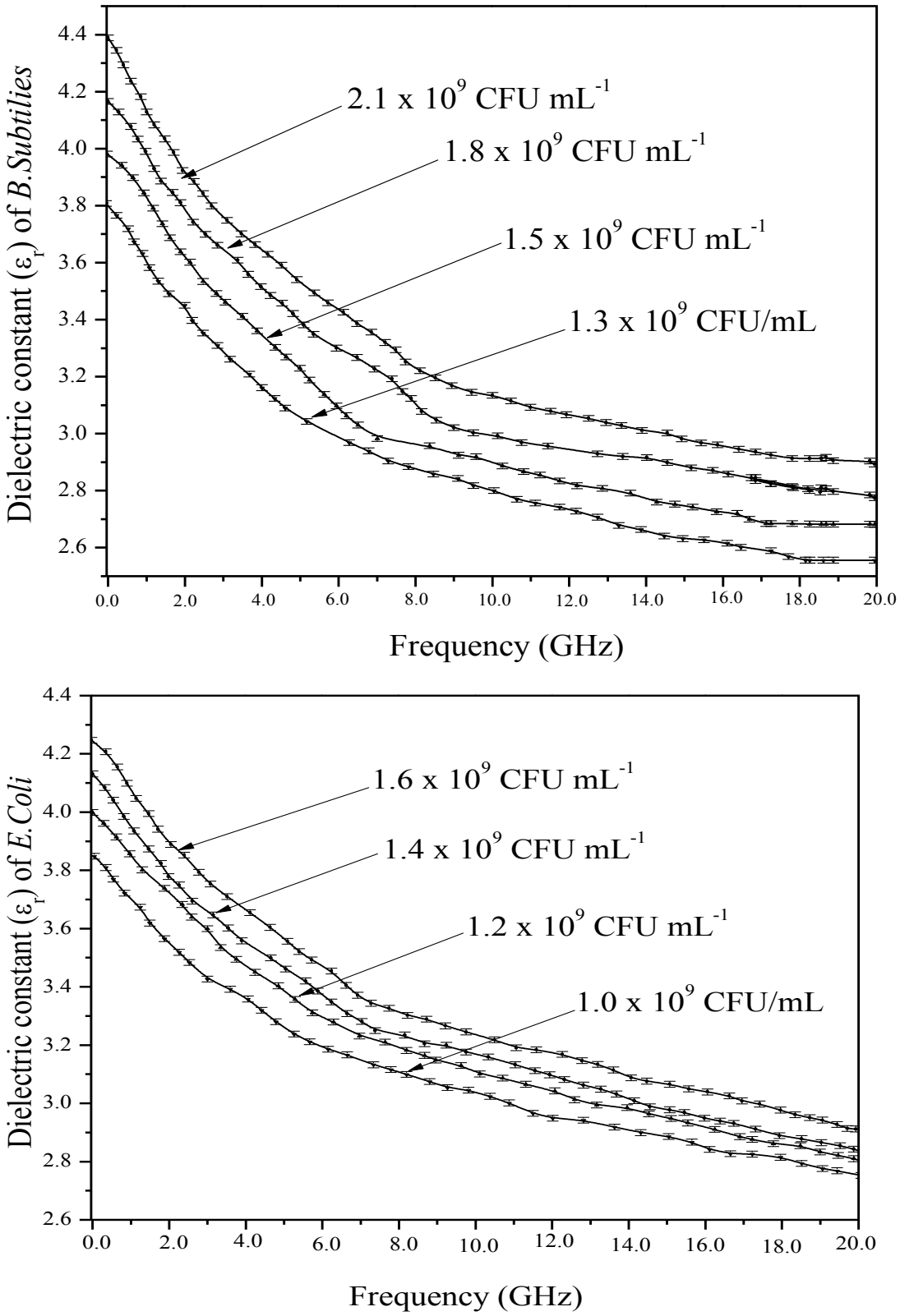
Dielectric constant (ε_r) of *B.Subtilies*
2.1 x 10^9 CFU mL^{-1}
1.8 x 10^9 CFU mL^{-1}
1.5 x 10^9 CFU mL^{-1}
1.3 x 10^9 CFU/mL
Frequency (GHz)
Dielectric constant (ε_r) of *E.Coli*
1.6 x 10^9 CFU mL^{-1}
1.4 x 10^9 CFU mL^{-1}
1.2 x 10^9 CFU mL^{-1}
1.0 x 10^9 CFU/mL
Frequency (GHz)

Figure 6

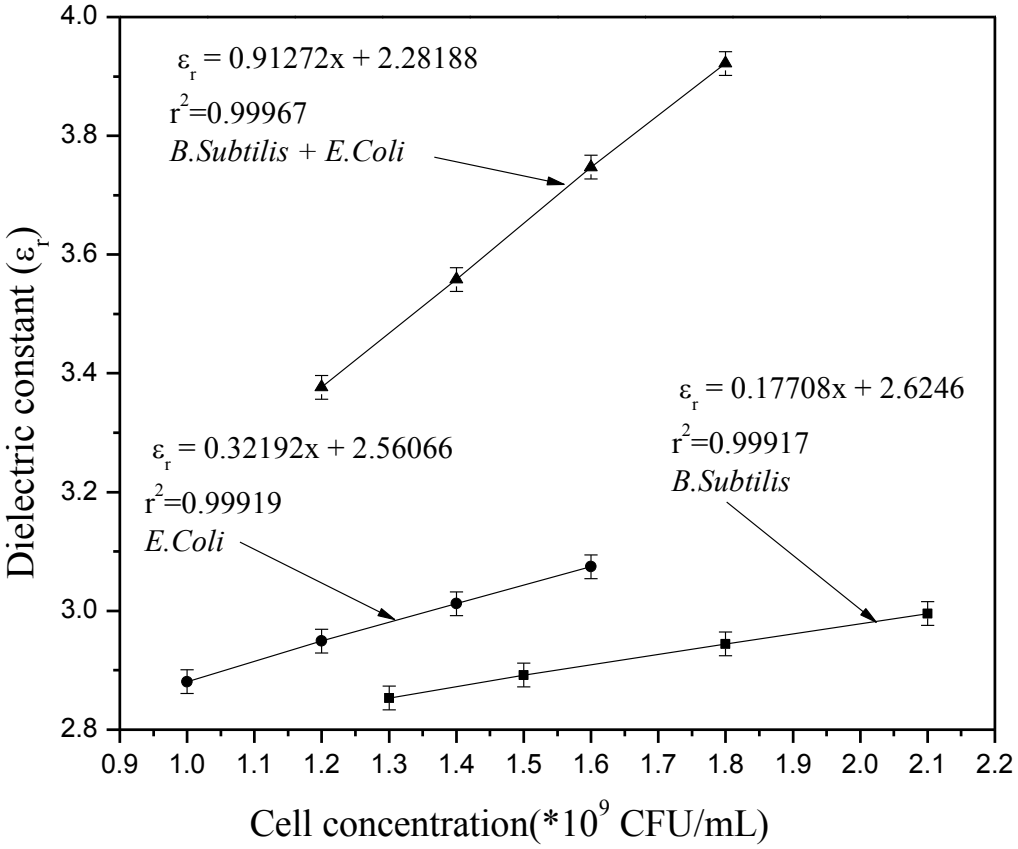
4.0
3.8
3.6
3.4
3.2
3.0
2.8
Dielectric constant (εr)
εr = 0.91272x + 2.28188
r2=0.99967
B.Subtilis + E.Coli
εr = 0.17708x + 2.6246
r2=0.99917
B.Subtilis
εr = 0.32192x + 2.56066
r2=0.99919
E.Coli
0.9
1.0
1.1
1.2
1.3
1.4
1.5
1.6
1.7
1.8
1.9
2.0
2.1
2.2
Cell concentration(*10^9 CFU/mL)

Figure 7

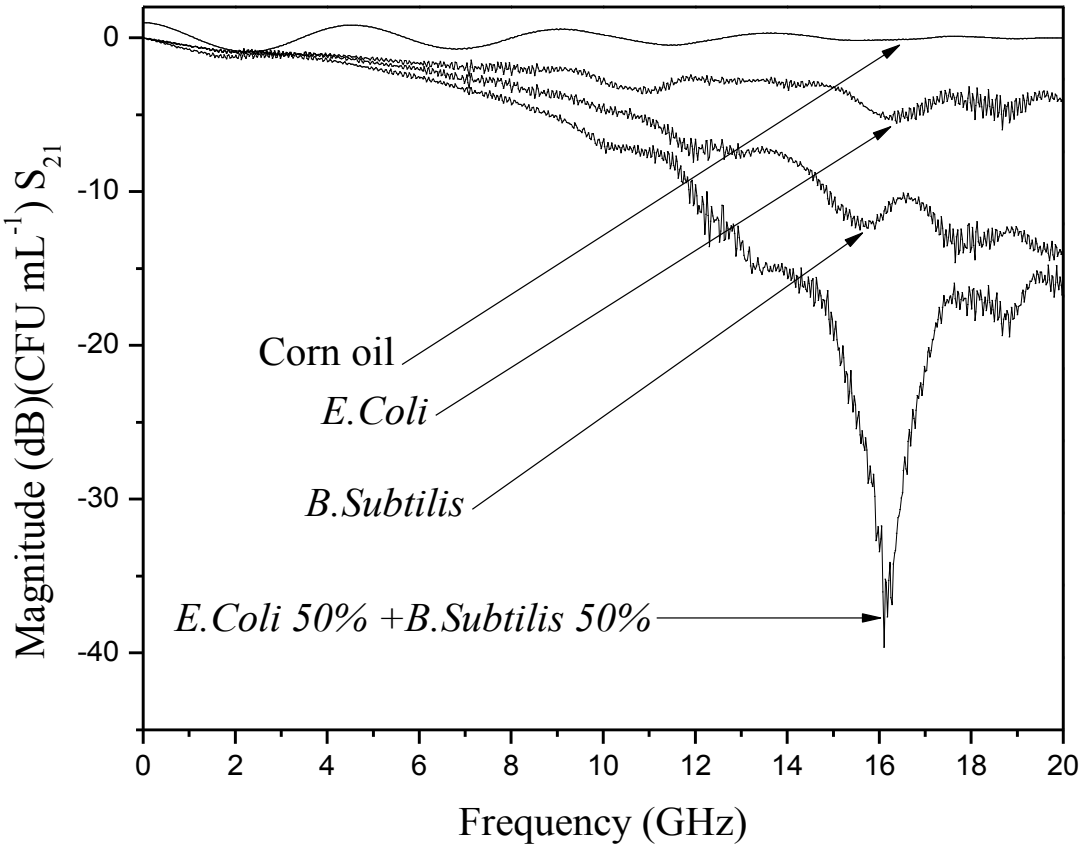
Magnitude (dB)(CFU mL-1) S21
Frequency (GHz)
Corn oil
E.Coli
B.Subtilis
E.Coli 50% +B.Subtilis 50%
0
-10
-20
-30
-40
0
2
4
6
8
10
12
14
16
18
20

Figure 8

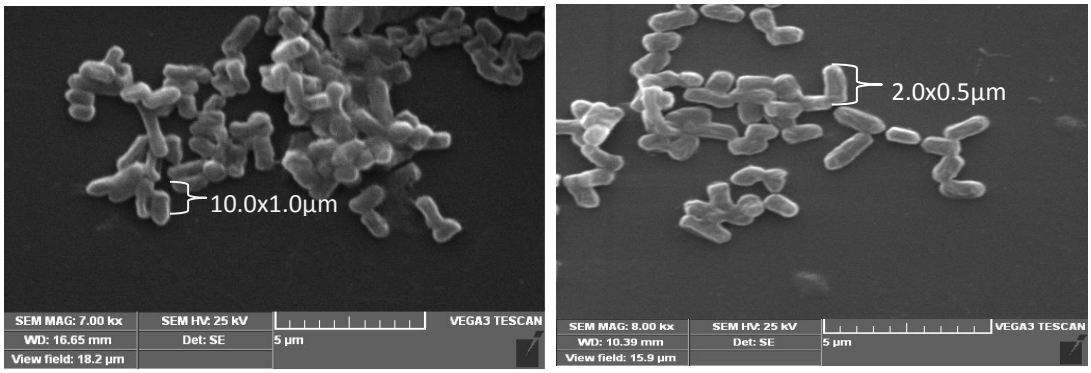

(a) *Bacillus Subtilis* (b) *Escherichia Coli*

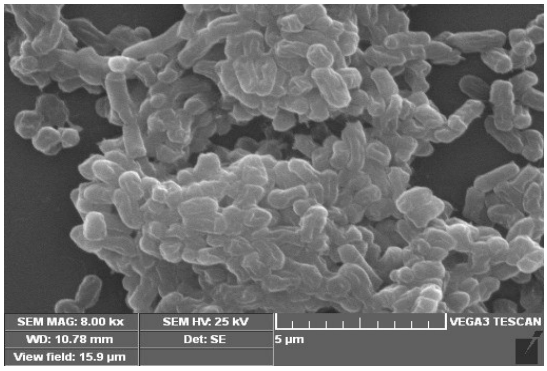

(c) *Escherichia Coli 50%+ Bacillus Subtilis 50%*

Figure 9

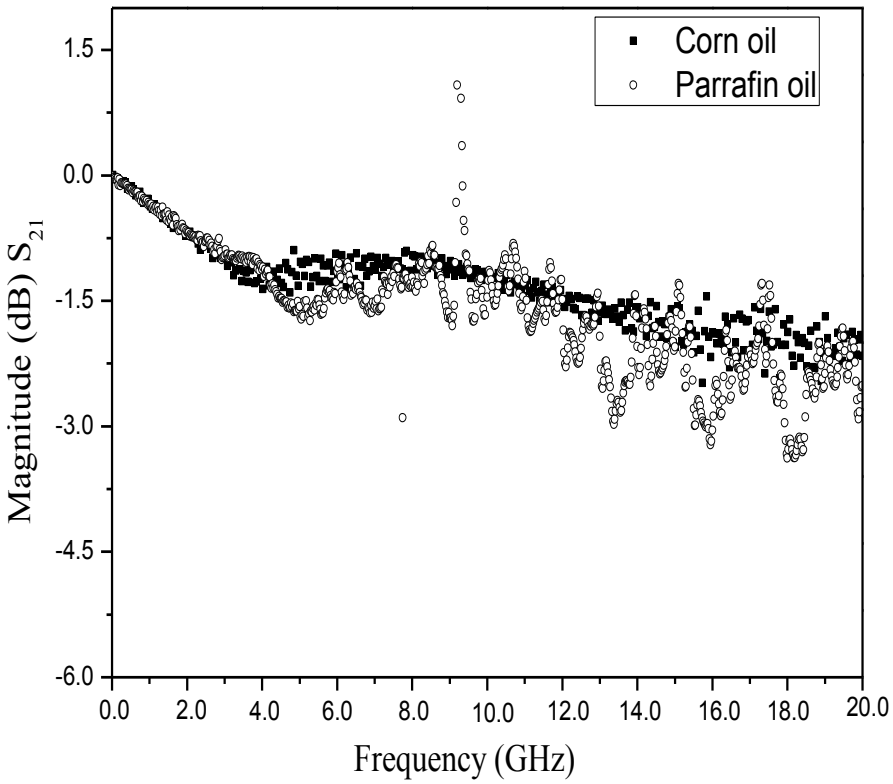

Figure 10